

Electron-phonon superconductivity and charge density wave instability in the layered titanium-based pnictide $\text{Ba}_{1-x}\text{Na}_x\text{Ti}_2\text{Sb}_2\text{O}$

Alaska Subedi

Centre de Physique Théorique, École Polytechnique, CNRS, 91128 Palaiseau Cedex, France

(Dated: October 2, 2012)

I present the results of first principles calculations of the phonon dispersions and electron-phonon coupling for $\text{BaTi}_2\text{Sb}_2\text{O}$. The phonon dispersions show a weak lattice instability near the zone corners that leads to a CDW phase. The calculations of the electron-phonon coupling reveal strong coupling, especially to the in-plane Ti modes. The total coupling is large enough to readily explain the superconductivity in this compound. As the Fermi surfaces are disconnected with different orbital character weights, this compound is likely to host a multiband superconductivity. The role of spin fluctuations in suppressing the superconducting T_c is also discussed.

PACS numbers: 74.25.Kc, 74.20.Pq, 74.70.-b

I. INTRODUCTION

The discovery of high temperature superconductivity in iron based compounds by Kamihara and coworkers¹ has increased interest and intensified efforts to find superconductors in new families of compounds. These efforts have focused on searching for materials with structural, electronic and magnetic properties similar to that of the iron or cuprate superconductors. In particular, the ideal candidates are thought to be materials with a layered structure that are in proximity to a spin density wave instability due to Fermi surface nesting like in the iron based superconductors or a Mott insulating phase due to strong on-site Coulomb repulsion as in the cuprates.

Recently, Doan *et al.* have reported superconductivity in $\text{Ba}_{1-x}\text{Na}_x\text{Ti}_2\text{Sb}_2\text{O}$ with a maximum T_c of 5.5 K.² Superconductivity in this compound has also been reported by Yajima *et al.* with a T_c of 1.2 K.³ In addition to the superconducting transition, there is also an anomaly at $T_a = 54$ K that manifests by showing strong features in the measurements of susceptibility, resistivity, and specific heat. The microscopic mechanism and the order parameter for this transition has not been determined, but it has been ascribed to either a charge density wave (CDW) or spin density wave (SDW) instability. Furthermore, the superconducting phase coexists with this CDW/SDW phase.

This compound occurs in a tetragonal structure with spacegroup $P4/mmm$ and consists of square planes of transition element Ti. The O atoms are placed alternately at the center of the Ti squares such that each Ti atom has two O nearest neighbors. The Sb atoms are placed above and below the center of the Ti squares that do not contain O atoms. The $\text{Ti}_2\text{Sb}_2\text{O}$ layers are stacked alternately with layers of Ba atoms along the c axis. This layered structure is similar to the iron based or cuprate superconductors as all of them have square planes of transition metal atom as a structural motif.

In addition, Singh has further highlighted similarities in the electronic and magnetic properties between $\text{BaTi}_2\text{Sb}_2\text{O}$ and the iron superconductors based on first

principles calculations.⁴ The Fermi surface shows substantial nesting and leads to an antiferromagnetic instability as in the case of iron superconductors. This nested Fermi surface is consistent with the results of Pickett on a similar compound $\text{Na}_2\text{Sb}_2\text{Ti}_2\text{O}$, although he was unable to find a magnetically ordered state.⁵ The electronic structure of $\text{Na}_2\text{Ti}_2\text{Sb}_2\text{O}$ was also studied by de Biani *et al.* using tight-binding calculations, and they also find substantial nesting in the Fermi surface that may lead to a CDW instability.⁶

In any case, the presence of a nested Fermi surface and antiferromagnetic instability in BaTi_2Sb_2 leads Singh to predict a spin fluctuation mediated superconductivity similar to that of the iron based superconductors.⁷ The pairing state is predicted to have a sign-changing s -wave symmetry that is different from that of the iron based superconductors. Furthermore, spin fluctuations are repulsive in the singlet channel and hence are strongly pair-breaking for the attractive electron-phonon interaction. Thus, it is reasonable to expect that the superconductivity in $\text{BaTi}_2\text{Sb}_2\text{O}$ is mediated by spin fluctuations, especially if the phase transition at $T_a = 54$ K that coexists with the superconducting phase is due SDW instability.

However, there are some differences between $\text{BaTi}_2\text{Sb}_2\text{O}$ and other superconductors near magnetism. The maximum $T_c = 5.5$ K of this compound is significantly smaller than that of the iron based or cuprate superconductors. This could be due to a small value of Stoner parameter for Ti⁸ or pair-breaking effects of electron-phonon interaction. It is worthwhile to note that Sr_2RuO_4 , which is purported to be an unconventional superconductor,⁹ also has a small T_c of 1 K.¹⁰ A more glaring difference is the very sensitive dependence of superconductivity on other constituent elements of the compound. A transition similar to the one in $\text{BaTi}_2\text{Sb}_2\text{O}$ is also seen in other members of the family that includes $\text{Na}_2\text{Ti}_2\text{Pn}_2\text{O}$ ($\text{Pn} = \text{As}, \text{Sb}$), $\text{BaTi}_2\text{As}_2\text{O}$, $(\text{SrF})_2\text{Ti}_2\text{Pn}_2\text{O}$ ($\text{Pn} = \text{As}, \text{Sb}$), $(\text{SmO})_2\text{Ti}_2\text{Sb}_2\text{O}$,^{11–18} but superconductivity has so far only been observed in Na doped $\text{BaTi}_2\text{Sb}_2\text{O}$. This is in contrast to iron superconductors which exhibit superconductivity for a wide variety of cations and pnictogens. In the cuprates,

superconductivity is also found for a wide variety of interlayer fillings that separate the CuO_2 layers. Even in the ruthenates, doping at the cation site or changing the interlayer spacing reveals various magnetic interactions. This suggests that magnetism and mechanism for superconductivity in doped $\text{BaTi}_2\text{Sb}_2\text{O}$ is quite different from other unconventional superconductors, and perhaps lattice instabilities and electron-phonon coupling play an important role.

In this paper, I present the results of first principles calculations that show presence of a CDW instability and a total electron-phonon coupling strong enough to yield a conventional superconductivity in $\text{BaTi}_2\text{Sb}_2\text{O}$. The phonon dispersions reveal a weak lattice instability near the Brillouin zone corners. This instability is associated with the elongation or compression of the Ti squares without an enclosed O such that the Ti squares with an O rotate either clockwise or counterclockwise by a small amount. I also find presence of strong electron-phonon couplings, especially near the zone corners. The total electron-phonon coupling $\lambda_{\text{ep}} = 1.28$ is large enough to readily explain the superconductivity in this material.

II. METHODS

The phonon dispersions and electron-phonon results presented here were obtained using density functional perturbation theory¹⁹ within the generalized gradient approximation of Perdew, Burke, and Ernzerhof²⁰ as implemented in the Quantum-ESPRESSO package.²¹ I used the experimental lattice parameters ($a = 4.11039 \text{ \AA}$, $c = 8.0864 \text{ \AA}$)³ but relaxed the internal Sb height parameter z_{Sb} . I obtained a value for $z_{\text{Sb}} = 0.2493$, which agrees well with both the experimental^{2,3} and calculated⁴ values. This is in contrast the underestimation from density functional calculations found in the iron based superconductors.⁷ This indicates that magnetism and/or lattice dynamics in $\text{BaTi}_2\text{Sb}_2\text{O}$ might be different from that of the iron based superconductors.

I used pseudopotentials that were generated with the electronic configurations $5s^25p^65d^06s^26p^0$, $3s^23p^24s^23d^1$, $5s^25p^35d^0$, and $2s^22p^43d^{-2}$, respectively, for Ba, Ti, Sb, and O. In particular, it was necessary to include the semi-core states to get the electronic structure in close agreement with the results of the full-potential calculations. I used the cut-offs of 60 Ry and 600 Ry for basis set and charge density expansions, respectively. An $8 \times 8 \times 4$ \mathbf{k} -grid was used for the Brillouin zone integration during the self-consistency. The dynamical matrices were also calculated on an $8 \times 8 \times 4$ \mathbf{q} -grid, while the double-delta integration in the calculation of the electron-phonon spectral function was done on a $24 \times 24 \times 12$ grid. I used the generalized full-potential method as implemented in the WIEN2k package²² to perform the relaxation of the internal coordinates of a $(\sqrt{2} \times \sqrt{2} \times 1)$ supercell. The muffin-tin radii of 2.4, 1.7, 2.4, and 1.7 Bohr were used for Ba, Ti, Sb, and O, respectively, and an $8 \times 8 \times 8$ \mathbf{k} -grid

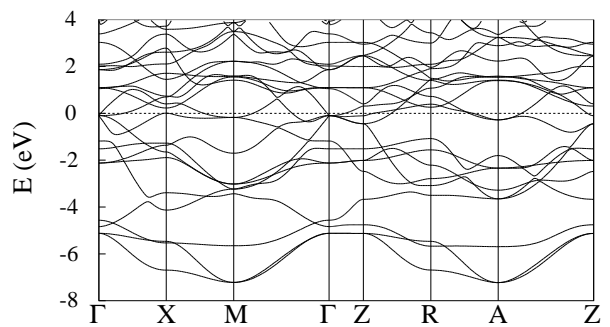


FIG. 1: Calculated GGA band structure of non-spin-polarized $\text{BaTi}_2\text{Sb}_2\text{O}$ in the underdistorted structure with experimental lattice parameters but relaxed internal coordinates.

was used for the Brillouin zone integration.

III. ELECTRONIC STRUCTURE

The electronic structure and magnetism of $\text{BaTi}_2\text{Sb}_2\text{O}$ has been well described by Singh.⁴ I summarize his results here for the sake of completeness. The band structure of this compound calculated using the pseudopotentials and plane-wave basis set is shown in Fig. 1. This agrees reasonably well with Singh's full-potential band structure that also includes the spin-orbit interaction. I also did full-potential band structure calculations without the spin-orbit coupling, and I find excellent agreement with the results from pseudopotential calculation. This shows that the pseudopotentials that I used are robust.

The three bands that lie between -7.3 and -4.7 eV have a dominant O $2p$ character, and another six bands with mostly Sb $5p$ character lie between -4.7 and -0.5 eV, relative to the Fermi energy. The bands near the Fermi level have mostly Ti $3d$ character with some hybridization with Sb $5p$ states, while the Ba $6s$ states are above the Fermi level. This suggests that Ti ions are nominally trivalent and are in d^1 state, although the actual electron count will be different due to some covalency with O $2p$ and Sb $5p$ states.

The Fermi surface (not shown; see Ref. 4) has a very two dimensional, square electron sheet around zone corner M with mixed Ti d_{z^2} , $d_{x^2-y^2}$, and d_{xy} characters. There is a three dimensional hole sheet around X with mostly Ti d_{z^2} with some admixture of $d_{x^2-y^2}$ and d_{xy} characters. Around the zone center there is a complex three dimensional electron sheet with mixed d_{z^2} and d_{xy} character. In the calculations without spin-orbit coupling, there is also a small electron sheet around the zone center that has a mixed character. Singh calculated the real part of the susceptibility within the constant matrix element approximation and finds peaks in the susceptibility due to substantial nesting between Fermi sheets, especially near the \mathbf{q} vector $(\frac{1}{2}, 0)$ ($2\pi/a$). In addition, there is

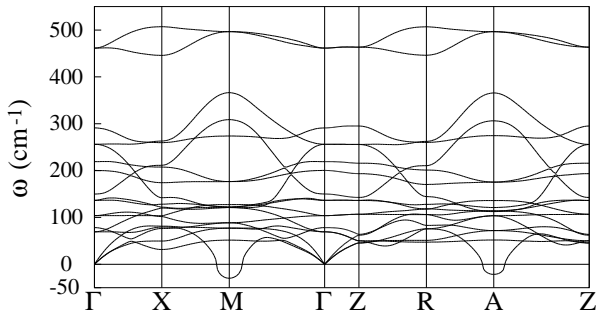


FIG. 2: Calculated GGA phonon dispersions of non-spin-polarized $\text{BaTi}_2\text{Sb}_2\text{O}$ in the underdistorted structure with experimental lattice parameters but relaxed internal coordinates. The imaginary frequencies are shown as negative.

also a smaller peak near the \mathbf{q} vector $(\frac{1}{2}, \frac{1}{2}) (2\pi/a)$. This could lead to magnetic instabilities at these \mathbf{q} vectors, although the height of the peaks could be diminished when the matrix element is explicitly taken into account in the calculation of the susceptibility. In any case, Singh finds that there is a magnetic instability at X that leads to a double stripe antiferromagnetic order with a doubling of the unit cell along either a or b axis with small moments of $0.2 \mu_B$ per Ti. Based on the proximity to the SDW instability, Singh predicts a spin fluctuation mediated superconductivity in doped $\text{BaTi}_2\text{Sb}_2\text{O}$ with a pairing state that has a sign-changing s -wave symmetry that is different from the one in the iron based superconductors.

IV. PHONONS AND ELECTRON-PHONON COUPLING

Although there seems to be a magnetic instability in $\text{BaTi}_2\text{Sb}_2\text{O}$, this does not preclude a competing lattice instability or an electron-phonon superconductivity. In this section, I show results that indicate that the anomaly at $T_a = 54$ K is due to a CDW instability and the electron-phonon coupling is large enough to readily explain the observed superconductivity.

The calculated phonon dispersions of $\text{BaTi}_2\text{Sb}_2\text{O}$ in the undistorted tetragonal structure with the experimental lattice parameters and relaxed internal coordinates are shown in Fig. 2, and the corresponding phonon density of states along with atomwise projections are shown in Fig. 3. A conspicuous feature of the phonon dispersions is the presence of an unstable mode around $M (\frac{1}{2}, \frac{1}{2}, 0)$ and $A (\frac{1}{2}, \frac{1}{2}, \frac{1}{2})$ indicating a CDW instability. The instability is weak with the maximum imaginary frequency of $30i \text{ cm}^{-1}$, suggesting a very shallow double well potential. The unstable mode has only in-plane Ti character, and the distortion corresponds to elongation or compression of the Ti squares without an enclosed O such that the Ti squares with O rotate either clockwise or counterclockwise by a small amount (see Fig. 4). I

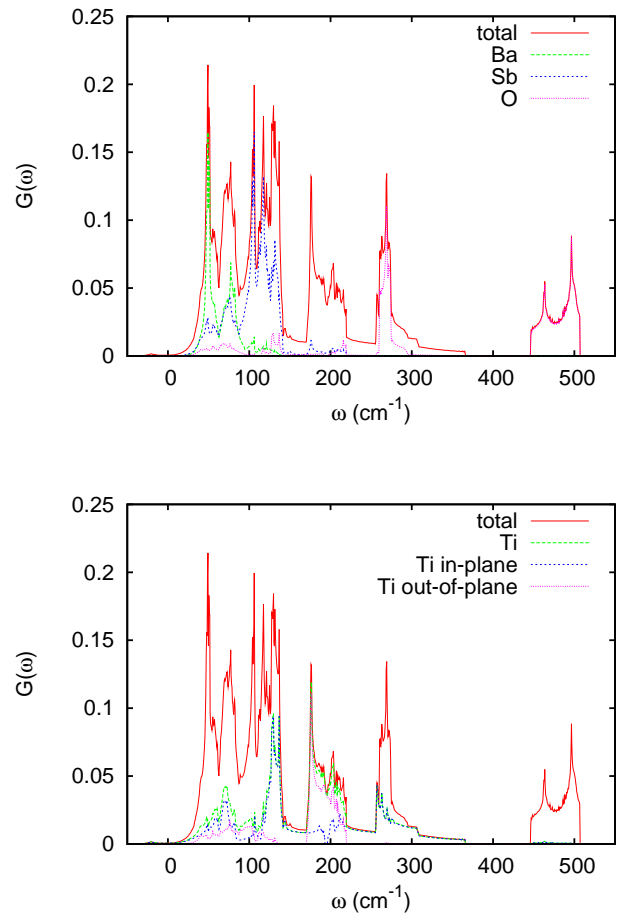


FIG. 3: (Color online) Top: Calculated GGA phonon density of states $G(\omega)$ along with atomwise projections on Ba, Sb, and O of non-spin-polarized $\text{BaTi}_2\text{Sb}_2\text{O}$ in the undistorted structure with experimental lattice parameters but relaxed internal coordinates. Bottom: Phonon density of states weighted by projections on Ti atom as well as its in-plane and out-of-plane characters.

also performed relaxation of a $(\sqrt{2} \times \sqrt{2} \times 1)$ super-cell with the full potential to check if the instability is a spurious effect of using pseudopotentials, and I again found a presence of this instability. The Ti ions get displaced by only 0.096 \AA from their original high-symmetry position. Although the Ti displacements are very small, I find a substantial reduction of the electronic density of states near the Fermi level with a reduction from a value of 3.88 eV^{-1} per formula unit in the undistorted case to a value of 2.83 eV^{-1} per formula unit in the CDW phase, as obtained from full-potential calculations without spin-orbit coupling. In addition, I also performed frozen phonon calculations on the $(\sqrt{2} \times \sqrt{2} \times 1)$ super-cell by displacing Ti atoms according to the eigenvector of the unstable phonon mode. As shown in Fig. 5, the potential is anharmonic with a minimum at 0.082 \AA , and the depth of the well is very shallow 14.5 cm^{-1} . Hence, it is not surprising that this CDW instability has so far

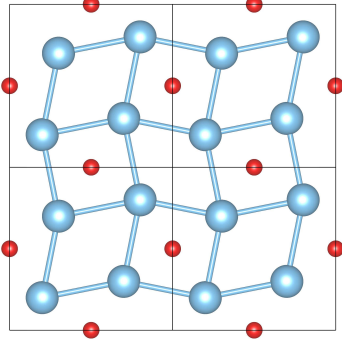


FIG. 4: (Color online) The distorted Ti plane in the CDW phase. The black grid shows the $(\sqrt{2} \times \sqrt{2} \times 1)$ supercell relative to the undistorted structure. The big (cyan) balls represent Ti and small (red) balls are O. The Ti displacements are exaggerated to make the distortions conspicuous.

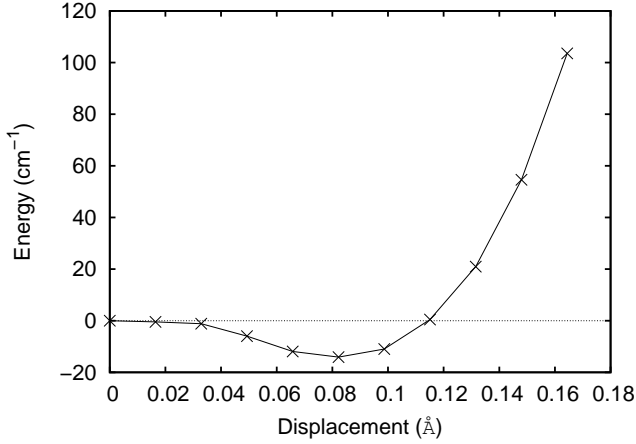


FIG. 5: Calculated anharmonic double-welled potential for the unstable mode obtained using frozen phonon method on a $(\sqrt{2} \times \sqrt{2} \times 1)$ supercell. The energy is given per formula unit.

been eluding detection.

Returning back to the phonon dispersions, the 18 modes of $\text{BaTi}_2\text{Sb}_2\text{O}$ in the undistorted structure extend up to 510 cm^{-1} . There is a manifold of 16 bands with mixed Ba, Ti, Sb, and out-of-plane O character extending up to 370 cm^{-1} , which is separated by a gap from two in-plane O modes between 445 and 510 cm^{-1} . Within the lower manifold of 18 bands, the Ba vibrations lie mostly within 100 cm^{-1} . The in-plane Ti character extends throughout this lower manifold, whereas the out-of-plane Ti modes are mainly confined to the two narrow bands within 165 and 225 cm^{-1} . Most of the Sb weight lies below 145 cm^{-1} , and the out-of-plane O modes lie between 255 and 295 cm^{-1} .

The strength of the interaction between electrons and phonons is generally given in terms of the Eliashberg

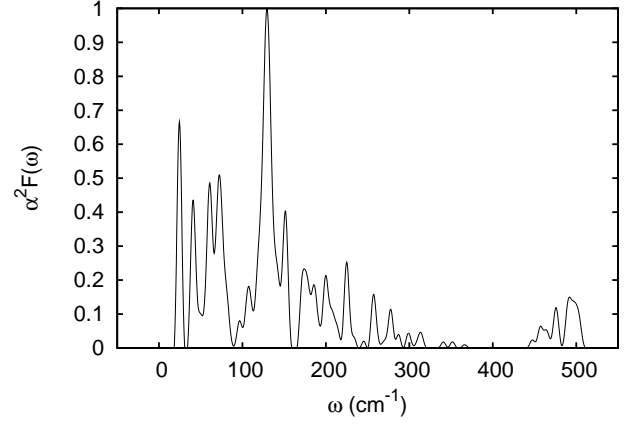


FIG. 6: Calculated Eliashberg spectral function of $\text{BaTi}_2\text{Sb}_2\text{O}$ in the underdistorted structure. The spectral weights for imaginary phonon frequencies are set to zero.

spectral function,

$$\alpha^2 F(\omega) = \frac{1}{N(E_F)} \sum_{\mathbf{k}, \mathbf{q}, \nu, n, m} \delta(\epsilon_{\mathbf{k}}^n) \delta(\epsilon_{\mathbf{k}+\mathbf{q}}^m) |g_{\mathbf{k}, \mathbf{q}}^{\nu, n, m}|^2 \delta(\omega - \omega_{\nu \mathbf{q}}), \quad (1)$$

where $N(E_F)$ is the electronic density of states at the Fermi energy, $\epsilon_{\mathbf{k}}^n$ is the electronic energy at wavevector \mathbf{k} and band index n , $\omega_{\nu \mathbf{q}}$ is the energy of a phonon with wavevector \mathbf{q} and branch index ν , and $|g_{\mathbf{k}, \mathbf{q}}^{\nu, n, m}|^2$ is the matrix element for an electron in the state $|n\mathbf{k}\rangle$ scattering to $|m\mathbf{k} + \mathbf{q}\rangle$ through a phonon $\omega_{\nu \mathbf{q}}$. The calculated Eliashberg spectral function for $\text{BaTi}_2\text{Sb}_2\text{O}$ is shown in Fig. 6. The spectral weight is spread through all the phonon frequencies, but it is specially enhanced at low frequencies below 90 cm^{-1} and between 100 and 160 cm^{-1} . I find that substantial part of the spectral weight comes from modes that involve in-plane Ti vibrations. This is reasonable as the states near the Fermi level are dominated by Ti d character. Furthermore, the inter-layer Ti-Ti distance is much larger than the intra-layer Ti-Ti distance, and the coupling to the out-of-plane Ti modes is much smaller, as one might expect.

The \mathbf{q} dependent total electron-phonon coupling $\lambda_{\mathbf{q}}$ ($= \int_0^\infty d\omega \alpha^2 F(\omega, \mathbf{q}) / \omega$) is plotted for the $k_z = 0$ plane of the Brillouin zone in Fig. 7. There are contributions to the electron-phonon coupling from throughout the Brillouin zone, but the magnitude of the electron-phonon coupling away from the zone center is much larger. In particular, the electron-phonon coupling is peaked near the wavevector $(\pi/a, \pi/a)$. Again, this is expected from the nesting between the Fermi sheets near the zone center and zone corners. Furthermore, since the disconnected Fermi sheets have different orbital character weights, the electron-phonon coupling on different Fermi sheets are likely to be different. Hence, this material is very likely to host a multiband superconductivity.

The total electron-phonon coupling constant is given

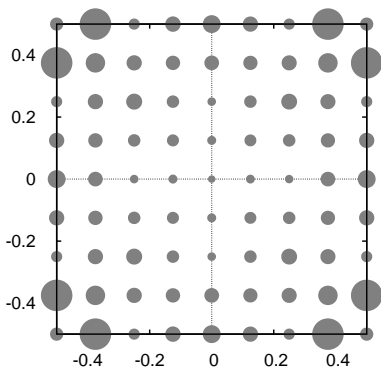


FIG. 7: Calculated \mathbf{q} dependent total electron-phonon coupling $\lambda_{\mathbf{q}}$ shown for the $k_z = 0$ plane of the Brillouin zone. The area of the circles is proportional to the magnitude of $\lambda_{\mathbf{q}}$. The unit of the axes is $2\pi/a$.

by $\lambda_{\text{ep}} = \sum_{\mathbf{q}, \nu} \lambda_{\mathbf{q}, \nu} = 2 \int_0^\infty d\omega \alpha^2 F(\omega) / \omega$. For $\text{BaTi}_2\text{Sb}_2\text{O}$, I obtain $\lambda_{\text{ep}} = 1.28$ with the logarithmically averaged frequency $\omega_{\text{ln}} = 65 \text{ cm}^{-1}$. (I obtain these numbers by setting the contribution from the imaginary frequencies to zero.) One can estimate the T_c within a single-band picture by inserting these numbers in the simplified Allen-Dynes formula,

$$T_c = \frac{\omega_{\text{ln}}}{1.2} \exp \left\{ - \frac{1.04(1 + \lambda_{\text{ep}})}{\lambda_{\text{ep}} - \mu^*(1 + 0.62\lambda_{\text{ep}})} \right\}.$$

With a value for the Coulomb pseudopotential parameter $\mu^* = 0.1$, I obtain $T_c = 9.0 \text{ K}$, which shows that the conventional electron-phonon picture readily explains the superconductivity in $\text{BaTi}_2\text{Sb}_2\text{O}$.

The electron-phonon calculations indicate that the superconductivity is of multiband strong-coupling nature with the predicted T_c of 9.0 K overestimating the experimentally obtained values of 5.5 K and 1.2 K.^{2,3} This discrepancy may be due to the pair breaking effects of spin fluctuations. The total coupling relevant for superconductivity is $\lambda = \lambda_{\text{ep}} - \lambda_{\text{sf}}$, where λ_{sf} is the contribution due to spin fluctuations. The presence of spin fluctu-

ations, as shown to exist in this compound by Singh,⁴ would therefore reduce the T_c .

V. CONCLUSIONS

In summary, I have presented the results of phonon dispersions and electron-phonon coupling calculations for $\text{BaTi}_2\text{Sb}_2\text{O}$. The phonon dispersions show a weak lattice instability around Brillouin zone corners that gives rise to a CDW instability. This CDW phase is likely the cause of the experimentally observed transition at 54 K that is seen in the measurements of susceptibility, resistivity, and heat capacity measurements.^{2,3} The distortions correspond to elongation or compression of the Ti squares without an enclosed O such that the Ti squares with O rotate either clockwise or counterclockwise by a small amount. This results in a $(\sqrt{2} \times \sqrt{2} \times 1)$ doubling of the unit cell.

The electron-phonon calculations reveal the presence of strong electron-phonon couplings, especially to the in-plane Ti modes. There are contributions to the total coupling from throughout the Brillouin zone, but the magnitude of the couplings are large away from the zone center. The electron-phonon coupling is peaked near the zone corners at wavevectors that would correspond to the nesting vectors between the Fermi sheets around the zone center and zone corners. The total electron-phonon coupling is $\lambda_{\text{ep}} = 1.28$, which gives an estimate of $T_c = 9.0 \text{ K}$ when inserted in the Allen-Dynes formula. This overestimates the experimentally observed values of T_c . This discrepancy may be due to the pair breaking effects of spin fluctuations, which has been shown to exist in this compound.⁴

VI. ACKNOWLEDGMENT

I gratefully acknowledge the use of computer cluster of the Anderson department at Max Planck Institute, Stuttgart, Germany.

¹ Y. Kamihara, T. Watanabe, M. Hirano, and Hideo Hosono, *J. Am. Chem. Soc.* **130**, 3296 (2008).

² P. Doan, M. Gooch, Z. Tang, B. Lorenz, A. Möller, J. Tapp, P. C. W. Chu, and A. M. Guloy, *J. Am. Chem. Soc.* (2012, in press).

³ T. Yajima, K. Nakano, F. Takeiri, T. Ono, Y. Hosokoshi, Y. Matsushita, J. Hester, Y. Kobayashi, and H. Kageyama, *J. Phys. Soc. Jpn.* **81**, 103706 (2012).

⁴ D. J. Singh, arXiv:1209.4668.

⁵ W. E. Pickett, *Phys. Rev. B* **58**, 4335 (1998).

⁶ F. F. de Biani, P. Alemany, E. Canadell, *Inorg. Chem.* **37**, 5807 (1998).

⁷ I. I. Mazin, D. J. Singh, M. D. Johannes, and M. H. Du, *Phys. Rev. Lett.* **101**, 057003 (2008).

⁸ O. K. Andersen, O. Jepsen, and D. Glözel, "Highlights of Condensed Matter Theory," Eds. F. Bassani, F. Fumi, and M. P. Tosi (North-Holland, Amsterdam) 1985, p. 59.

⁹ T. M. Rice and M. Sigrist, *J. Phys. Condens. Matter* **7**, L643 (1995).

¹⁰ Y. Maeno, H. Hashimoto, K. Yoshida, S. Nishizaki, T. Fujita, J. G. Bednorz, and F. Lichtenberg, *Nature* **372**, 532 (1994).

¹¹ A. Adam and H.-U. Schuster, *Z. Anorg. Allg. Chem.* **584**, 150 (1990).

¹² E. A. Axtell, III, T. Ozawa, S. M. Kauzlarich, and R. R. P. Singh, *J. Solid State Chem.* **134**, 423 (1997).

¹³ T. C. Ozawa, R. Pantoja, E. A. Axtell, III, S. M. Kauzlarich, J. E. Greedan, M. Bieringer, and J. W. Richard-

- son, Jr., J. Solid State Chem. **153**, 275 (2000).
- ¹⁴ T. C. Ozawa, S. M. Kauzlarich, M. Bieringer, and J. E. Greedan, Chem. Mater., **13**, 1804 (2001).
 - ¹⁵ T. C. Ozawa and S. M. Kauzlarich, J. Cryst. Growth **256**, 571 (2004).
 - ¹⁶ R. H. Liu, D. Tan, Y. A. Song, Q. J. Li, Y. J. Yan, J. J. Ying, Y. L. Xie, X. F. Wang, and X. H. Chen, Phys. Rev. B **80**, 144516 (2009).
 - ¹⁷ X. F. Wang, Y. J. Yan, J. J. Ying, Q. J. Li, M. Zhang, N. Xu, X. H. Chen, J. Phys.: Condens. Matter **22**, 075702 (2010).
 - ¹⁸ R. H. Liu, Y. A. Song, Q. J. Li, J. J. Ying, Y. J. Yan, Y. He, and X. H. Chen, Chem. Mater. **22**, 1503 (2010).
 - ¹⁹ S. Baroni, S. de Gironcoli, A. Dal Corso, and P. Giannozzi, Rev. Mod. Phys. **73**, 515 (2001).
 - ²⁰ J. P. Perdew, K. Burke, and M. Ernzerhof, Phys. Rev. Lett. **77**, 3865 (1996).
 - ²¹ P. Giannozzi, S. Baroni, N. Bonini, M. Calandra, R. Car, C. Cavazzoni, D. Ceresoli, G. L. Chiarotti, M. Cococcioni, I. Dabo *et al.*, J. Phys.: Condens. Matter **21**, 395502 (2009).
 - ²² P. Blaha, K. Schwarz, G. Madsen, D. Kvasnicka, and J. Luitz, “WIEN2k, An Augmented Plane Wave + Local Orbitals Program for Calculating Crystal Properties” (K. Schwarz, Tech. Univ. Wien, Austria) (2001).